Contamination Control for Ultra-Sensitive Life-Detection Missions

Jennifer L. Eigenbrode[1]*, Robert Gold[2], John S. Canham[1,3], Erich Schulze[2], Alfonso F. Davila[4], Antonios Seas[1], Therese Errigo[1], Faith Kujawa[2], David Kusnierkiewicz[2], Charles Lorentson[1] and Christopher McKay[4]

[1]NASA Goddard Space Flight Center, Greenbelt, MD, United States, [2]Applied Physics Laboratory, Johns Hopkins University, Laurel, MD, United States, [3]Peraton, Inc., Beltsville, MD, United States, [4]NASA Ames Research Center, Mountain View, CA, United States

A key science priority for planetary exploration is to search for signs of life in our Solar System. Life-detection mission concepts aim to assess whether or not biomolecular signatures of life are present, which requires highly sensitive instrumentation. This introduces greater risk of false positives, and perhaps false negatives. Stringent science-derived contamination requirements for achieving science measurements on life-detection missions necessitate mitigation approaches that minimize, protect from, and prevent science-relevant contamination of critical surfaces of the science payload and provide high confidence to life-detection determinations. To this end, we report on technology advances that focus on understanding contamination transfer from pre-launch processing to end of mission using high-fidelity physics in the form of computational fluid dynamics and sorption physics for monolayer adsorption/desorption, and on developing a new full-spacecraft bio-molecular barrier design that restricts contamination of the spacecraft and instruments by the launch vehicle hardware. The bio-molecular barrier isolates the spacecraft from biological, molecular, and particulate contamination from the external environment. Models were used to evaluate contamination transport for a designs reference mission that utilizes the barrier. Results of the modeling verify the efficacy of the barrier and an in-cruise decontamination activity. Overall mission contamination tracking from launch to science operations demonstrated exceptionally low probability on contamination impacting science measurements, meeting the stringent contamination requirements of femtomolar levels of compounds. These

Abbreviations: APL/JHU, applied physics aboratory, john hopkins university; ARC, ames research center; BET, brunauer, emmett, teller [theory]; CFD, computational fluid dynamics code for simulating multi component flows, mixing, diffusion and chemical reaction; CNTM, contamination requirement identifier (SM); COSPAR, committee on space research; CTSP, contamination transport simulation program; DRM, design reference mission; ECS, environmental control system; ELSAH, enceladus life signatures and habitability mission concept; evaporation enthalpy, number molecules evolved per unit time; FED STD Class 100, room or vessel having 100 particles per ft^3 where the particles are ≤0.5 μm; GCMS, gas chromatography mass spectrometry; GSFC, goddard space flight center; GR, ground rule identifier (SM); HEPA filter, high efficiency particulate air filter; ISO Class 5, room or vessel having 100 particles per ft^3 where the particles are ≤0.5 μm; LoD, limit of detection; LSP, NASA's launch services program; LV, launch vehicle; LVE, launch vehicle environment; NVR, non-volatile residue; OBJ, objective identifier (SM); PAC, percent area coverage; PP, planetary protection; RTG, radioisotope thermoelectric generator; SSM, specified by specific mission; SNR signal-to-noise ratio; TOC, total organic carbon.

advances will enable planetary missions that aim to detect and identify signatures of life in our Solar System.

INTRODUCTION

Robotic missions that aim to detect, identify, and measure possible biomolecules, determine signatures-of-life parameters, and ultimately determine whether life exists or has existed in an extraterrestrial planetary environment (McKay et al., 2013; Reh et al., 2016; Hand et al., 2017; Eigenbrode et al., 2018; Turtle et al., 2018; Williford et al., 2018; MacKenzie et al., 2021) must implement steps that mitigate the risks of false positive detections. Possible sources of false positives in missions evaluating signatures of life (herein referred to as "life-detection missions") include contaminants such as terrestrial cells, cellular parts, biomolecules, and anthropogenic interferences. The inadvertent presence of such contaminants on flight instruments and supporting sampling systems, collectively termed the science payload, are the greatest concern, as they could compromise, or invalidate, the interpretation of a positive life-signature experiment.

The importance of contamination control has gained relevance in the context of astrobiology missions primarily for two related reasons. First, is the realization that signatures of life such as biomolecules in other planetary bodies of the Solar System are likely to be present at very low abundances, and therefore might be easily obscured by small amounts of terrestrial contaminants. Second, prompted by the expected low abundances of biogenic compounds, existing flight instruments capable of detecting biomolecular signatures have achieved exquisite levels of detection (LoD) and can measure target compounds at pico-to femtomole levels (Hand et al., 2017; MacKenzie et al., 2021) the mole equivalent to the molecular content in 1–10 bacterial cells. However, the trade-off of ultra-sensitivity is the risk of detecting contaminants, potentially preventing, obscuring, or confounding the detection of native molecules (false negative) or causing false positive detections. Therefore, the performance of ultra-sensitive instruments for detecting life signatures is tightly link to the acceptable levels and types of contaminants on their surfaces (understanding that absolute lack of contamination is not possible), as they are both required to meet mission science objectives.

Performance parameters of flight instruments are captured in the form of measurement and instrument requirements (often denoted by NASA as Level-1 requirements). Level-1 requirements establish the level of performance that the science payload must meet to achieve the mission's scientific goals and are defined in the early stages of mission development. Examples of important Level-1 requirements typically include sample volumes, instrument LoD, detectable compounds, and instrument signal-to-noise ratios (SNR). Contamination control strategies ensure that the science payload can meet the Level-1 requirements without interference from terrestrial sources. The ubiquity of terrestrial biochemicals in every environment of Earth exasperates the challenge to controlling contamination of spacecraft hardware. Stringent science-derived contamination requirements that guarantee the science return of the science payload's performance necessitate innovations in mitigation approaches that minimize, protect from, and prevent contamination of critical surfaces, thus enabling successful detections and identifications of compounds indigenous to the samples acquired and supporting science investigations at hand.

Here, we present the results of a technology study that addresses two existing gaps in contamination control for ultra-sensitive life-detection missions: 1) preserving the ultraclean spacecraft, with its science payload elements, in a verified state during LV processing and launch, and 2) advancing the fidelity of particulate and molecular contamination transport models to account for fluid dynamics of the launch vehicle environment (LVE) and monolayers or less of molecules on ultraclean spacecraft surfaces to verify cleanliness levels at different stages of the mission. Thorough evaluation of trades in designs resulted in two new technologies that address the challenges: 1) a purged spacecraft barrier for protection until the spacecraft is no longer exposed to sources of terrestrial contamination, and 2) a new high-fidelity physics, numerical model for testing the efficacy of the barrier to protect the spacecraft and of a decontamination activity (in-cruise bakeout of sample collector) to determine the overall cleanliness of the sample pathway at the start of science operations.

Background
Planetary Protection and Contamination Control

Missions to astrobiological sites require high sterility for planetary protection. However, life-detection missions need additional extreme molecular cleanliness since traces of dead bio-molecular compounds may still confuse the search for life. Contamination control in planetary missions has largely focused on meeting Planetary Protection bioburden requirements, i.e., the abundance of viable cells or spores on spacecraft surfaces (National Academies of Sciences, Engineering, and Medicine, 2018; 2020). Ultimately, planetary mission must comply with bioburden levels specified by the COSPAR Planetary Protection rules, which are designed to minimize the probability of forward transfer of viable organisms to potentially habitable environments on other worlds (COSPAR Policy on Planetary Protection, 2020; see rules) and to the sample materials to be analyzed. Importantly, science-derived contamination requirements may be more stringent than Planetary Protection bioburden requirements.

Notably, planetary protection protocols typically used to reduce bioburden levels (e.g., dry heat microbial reduction), can still leave behind cellular fragments or cellular contents,

which become potential sources of organic chemical contamination. Other potential sources of contaminants include inadvertent human manipulation or exposure of the spacecraft to a contaminating environment, such as the interior of a rocket (LV) fairing. Such contamination can potentially interfere with science measurements particularly if present along the sample path (COSPAR Policy on Planetary Protection, 2020; for category IVB and V missions to targets of interest in "understanding the process of chemical evolution or the origin of life").
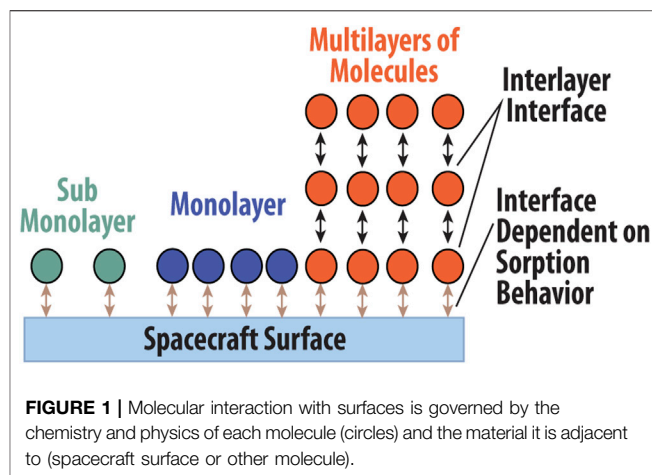
Launch Vehicle Environment

This paper addresses the particular concern of a possible transfer of particles and organic compounds from the rocket fairing (provided by a LV vendor) to a clean spacecraft (delivered and maintained by NASA), especially to critical surfaces along the sample path within the instrument systems. LV processing and launch operations pose significant contamination risks for all sensitive missions (*e.g.,* inadvertent contaminant transfer from personnel working in the fairing, limited cleanliness monitoring and recleaning capability, contamination events, non-redundant environmental systems, pressurization failures, launch window limitations).

Modifying LV processing to prevent such contamination increases both launch costs and risks; therefore, less invasive methods for cleaning and protecting spacecraft surfaces are common practice. For example, tape lifts, swabs of surfaces for non-volatile residues (NVR), visual inspections, witness samples, etc. are employed to certify that contaminant levels are verified in the LVE. Once verified, critical surfaces are protected from volatile outgassing and recondensation, as well as particulate transfer during other launch operations using barriers, covers, purges, cleaning of the fairing, environmental controls, etc. While these contamination control practices have been successfully implemented in planetary missions (*e.g.,* Viking landers, Mars Science Laboratory Curiosity rover, and Mars2020 Perseverance rover with sampling cache for a future Mars Sample Return), they have not yet been validated for modern-day, ultra-sensitive *in situ* missions aiming to search for signatures of life including those of extant life.

Contamination Control Engineering Principles

Contamination control engineering implemented effectively achieves cleanliness that will not degrade the performance of science payload. Every mission will have mission-specific, science-derived contamination requirements that depend on what signal must be measured, the sensitivity and resolution of the detectors, and the selectivity toward other signals. Different levels of cleanliness will be required for different instruments systems and their subsystems.

Traditionally, cleanliness requirements are verified at launch and then the sample path is protected until science operations at the destination ensue (see *Launch Vehicle Environment*). In this traditional approach, there is no direct measure of contaminant transfer from other surfaces on or outside the spacecraft. Nor is there evaluation of different types of particles or molecules. Rather it is assumed that the bulk particulate and molecular

FIGURE 1 | Molecular interaction with surfaces is governed by the chemistry and physics of each molecule (circles) and the material it is adjacent to (spacecraft surface or other molecule).

contamination has a single specific impact on science. Despite the effectiveness of traditional, well-proven techniques and operations for many types of planetary missions, these methods alone are insufficient for meeting the stringent contamination requirements (such as picomolar to femtomolar levels of biomolecules present as a monolayer or sub-monolayer on surfaces, **Figure 1**) of missions seeking signatures of life. Furthermore, traditional contamination transport modeling only tracks pressure/temperature-driven evaporation and deposition of initial bulk contamination using view factors and simple ray tracing. Applying such models becomes a computationally intractable problem for low levels of particles and molecules. When dealing with extremely clean systems, models based on bulk behavior can significantly diverge from the actual contaminant behavior.

Instead, for ultra-sensitive life-detection missions, contamination levels ought to be verified by back-tracking potential contamination transport during each mission phase and between designated hardware points, starting with Level-1 science requirements at and during science operations. This suggested change in contamination control engineering principle is enabled by 1) using flight instruments, which offer the best verification testing if available, or similar instruments capable of detecting acceptable contaminant types and levels, and 2) high-fidelity contamination transport modeling for mission phases that are likely to experience contamination transport to or from critical surfaces in the science payload. Improved verification and modeling combined with existing cleaning techniques that establish ultraclean surfaces provides a more comprehensive strategy for meeting stringent contamination requirements for mission science investigations of biological potential.

MATERIALS AND METHODS

Enceladus-Plume Design Reference Mission for Testing Mitigation Approaches

Each life-detection mission concept is unique in its destination, nature of the targeted samples, sampling methods, target

compounds, and operations. It was beyond the scope of this technology study to address all these possibilities; however, some of the study's innovations are widely applicable to all cases and could be leveraged in future mission designs.

For this study, we used the New Frontiers-class Enceladus Life Signatures and Habitability mission (ELSAH) as the design reference mission (DRM) (Eigenbrode et al., 2018). ELSAH requires very stringent contamination control, making it an ambitious test case for developing contamination prevention and mitigation strategies. Similar missions seeking signatures of modern or extant life on Enceladus, Mars, or Europa are likely to have comparative contamination requirements, but they will differ in the mission-specific details. The DRM consists of an orbiter that flies through the plume of Enceladus multiple times at low altitude to collect and analyze plume material. The primary science objective of the mission is to search for chemical signatures of life in ocean materials sampled in the plume. Specific DRM features (e.g., spacecraft configuration, a covered, 1-m^2 aperture cone-shaped sample collector (Adams et al., 2018), and a sample collector bakeout operation during cruise) were used in this study as the basis for evaluating the overall effectiveness of a mitigation strategy that applies the new engineering principles (*Contamination Control Engineering Principles*) and new technologies. Cassini mission results were used to constrain plume and ice particle characteristics (**Supplementary Material**).

Sample Collector and Purge

From the DRM, an extremely clean gas purge (*Purge Gas Purity*) at atmospheric pressure is required for the covered sample collector prior to launch. During integration to the LV, the collector at about 20°C may experience minor contamination loss. The evaporation rates of volatile contaminants will be limited by near-surface stagnation zones that decrease the rate of evolution of molecules from the surface. The purpose of the purge at this stage is primarily to minimize the incursion of external contamination into the collector prior to launch. The incursion of contamination into the collector is further limited by a labyrinth seal between the collector and its cover. Details of this seal are provided in **Supplementary Material**. During launch, there will be gas flow from the interior of the collector outward. The ascent venting will result in viscous gas flow out of the collector, providing some additional protection during ascent. The purge flow and depressurization limit the particulate and microbial contamination of the interior of the collector until the purge gas is completely exhausted, which occurs in the vacuum of space several hundred kilometers above Earth's surface.

The collector will be tightly covered during the initial mission phase. During this phase, the spacecraft will be at less than one astronomical unit from the Sun, where the collector may reach a temperature of up to 70°C. The collector is designed to be nearly isothermal, mitigating the potential for cold spot deposition and concentration. Due to the restrictive nature of the cover/collector joint, the movement of any contamination in or out of the collector will be negligible. There may be some redistribution of the surface molecular contamination within the collector assembly. This redistribution will not have any significant impact on the contaminant behavior.

The collector remains tightly closed during the cruise toward Enceladus. The temperature of the spacecraft surfaces and collector are expected to cool to approximately −140°C. The rate of evaporation transfer of material is expected to reduce by a factor of a trillion, assuming a two-fold reduction in transport for a temperature reduction of 10°C, which is an estimate based upon the average heat of vaporization for organic molecules from a surface. After passing Titan, the cover of the collector opens, and heats to about >250 °C for approximately 1 hour to degrade and volatilize any last residual terrestrial contaminants from this critical component of the science payload.

Target Compounds

The primary targeted compounds of the DRM were amino acids and hydrocarbon lipids (*e.g.,* fatty acids or *n*-alkanes). Sample volume collected was assumed to be 2–50 μL. Required LoDs were assumed to be at the femtomolar level for each compound of interest. Requirements for acceptable contamination levels are based on achieving a SNR of 3:1[1]. Other mission concepts may require higher than femtomolar level contamination tolerances for target molecules; however, the DRM serves as a stress-case to help support development of contamination prevention and mitigation strategies that could be applied broadly to all missions that are ultra-sensitive to contaminants.

Determination of contamination levels for science-designated target molecules started with instrument performance specifications (**Table 1**). The study then considered possible particulate and molecular contamination transfer from the sample collector to the sample path and to instrument detectors; spacecraft outgassing and particulate transfer to the collector; an in-cruise bakeout of the collector; and particulate and molecular contamination transfer from the LV fairing to the spacecraft at launch.

Specifications Development

The specification (or requirements) development process was guided by objectives and ground rules. Within this framework, three levels of requirements were determined for the technology study (for details: **Supplementary Material**). Basic science requirements known as Level-1s in NASA missions, were based on the DRM's science measurements, instrument performance specifications and mission requirements regarding sampling (**Table 1**), a PP requirement that ensures compliance with NASA PP policy (NPD 8020.7G), and LVE Definitions. Level-2 (L2) requirements for contamination control and barrier design requirements flowed from multiple sources (**Figure 2**). Level-3 (L3) requirements captured standard and non-standard launch services; mission-unique launch services; and spacecraft modifications. Objectives, Ground rules, LVE

---

[1]A SNR of 3:1 is based upon three times the root means square standard deviation of the noise. Assuming a normal noise distribution, this provides a 99.97% probability that the signal is not a noise variation, but an actual signal.

TABLE 1 | Level-1 science requirements for this study based on expected instrument performance that assumes 20% improvement on measurement requirements of the DRM (*Enceladus-Plume Design Reference Mission for Testing Mitigation Approaches*).

ID	Measurement requirements	Expected instrument performance
SCI-1	The mission shall be able to measure individual amino acid structures present at ~300 fmol with a SNR of 3:1	The science payload shall have a LoD for individual amino acid structures of ~240 fmol with a SNR of 3:1
SCI-2	The mission shall be able to measure individual C11-C22 lipid hydrocarbons present at ~60 fmol with a SNR of 3:1	The science payload shall have a LoD for individual C11-C26 lipid hydrocarbons of ~48 fmol with a SNR of 3:1

FIGURE 2 | Contamination control study requirements flow diagram. (Req'ts: requirements).
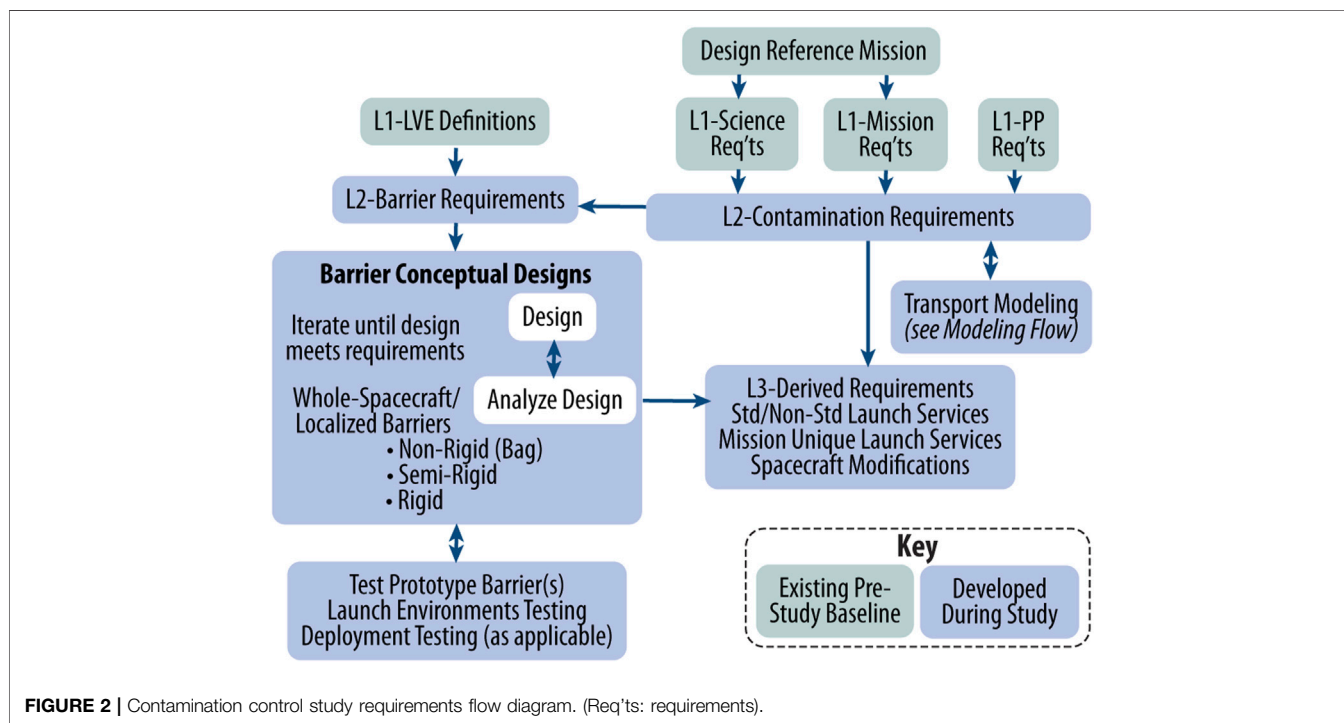
definitions, and L2-L3 requirements are provided as tables in **Supplementary Material**.

Science Requirements

The L1 science requirements for this study were traced to the DRM's science objective that aims to determine the biological potential of a subsurface ocean at Saturn's moon Enceladus, including detection of life signatures. These L1 science requirements include instrument requirements with some margin (i.e., instrument performance specifications) and mission requirements and were based on the expected abundances of amino acids and lipid hydrocarbons in the Enceladus Ocean, sampled by an orbiter from a cryovolcanic plume. These values are published elsewhere (MacKenzie et al., 2021), and assume a total organic content (TOC)[2] in the Enceladus Ocean of 30 µM (similar to the value assumed for Europa in Hand et al., 2017). For

simplicity, expected amino acid and lipid abundances were defined in moles and referenced to instrument LoD and SNR, assuming a minimal sample volume of 2 µL obtained after one flythrough of the Enceladus plume (**Table 1** in Porco et al., 2017). Since many high-TRL instruments can make the measurements and their capabilities differ, instrument performances were assumed to offer at least 20% improvement over LoD requirements while maintaining at least a 3:1 SNR.

Level-2 Contamination Requirements

The L2 contamination requirements define the types of contaminants that are of concern, and the allowable levels of these contaminants that may be present and still ensure the science objectives are met. These requirements were derived from the mission requirements expected instrument performance (**Table 1**), mission requirements for sampling, and NASA PP policy, as well as the contamination transport modeling results that defined such lower-level requirements as allowable materials (for spacecraft, fairing, processing facilities), bakeouts, purge gas purity, etc. (**Figure 2**). Contamination requirements would normally flow into Contamination

---

[2]Expected amino acid abundance assumes a ratio of amino acids to TOC = 1:200 (similar to Earth's oceans); and expected lipid hydrocarbon abundance assumes a ratio of lipids to amino acids = 1:5 (similar to Earth's oceans).

Control Plans and Materials and Processes Control Plans of mission design, but in the case of this study, these details were captured as Level 3 derived requirements.

Level-2 Barrier Design Requirements

Early in the study it was determined that a barrier that fully enclosed the spacecraft would be the optimal solution to prevent transfer of particles and organic compounds to critical surfaces along the sample path, during prelaunch activities at the launch facility, and through launch. The barrier would self-deploy in the space environment at the beginning of the cruise phase, liberating the clean spacecraft. Other possible solutions considered, such as localized barriers around the sampling system, were deemed likely insufficient and more complex to implement. The design concept for the full barrier was required to be able to support a wide range of missions including ones requiring radioisotope thermoelectric generators (RTGs). Other driving requirements and goals for the design concept were largely traceable to L1 LVE definitions and L2 contamination requirements.

Barrier design requirements included specifications for material, mass, dimensions, internal pressure, LV constraints, launch activities, and how the seams open to release the spacecraft. Payload processing and operability considerations, such as the ability to repair a tear in the barrier once it is in place around the spacecraft, were also identified in the requirements. The barrier materials need to survive high temperatures from a sterilizing procedure and RTG proximity. Other requirements included use of low outgassing materials on the spacecraft facing surfaces, very low purge gas leakage, accommodating late RTG mounting, being repairable from outside of the barrier, being able to withstand launch ascent venting, and being able to be reliably open on command in a space environment. Installing a barrier around a spacecraft that will self-deploy in a space environment presented several unique challenges and spacecraft design constraints. These spacecraft design constraints that limit placement of some spacecraft hardware (e.g., geometry constraints, thermal constraints, and accessibility constraints) were taken into consideration for the DRM. This section is a summary of the barrier design requirements table provided in **Supplementary Material**.

Purge Gas Purity

The contamination requirements necessitate purge gas purity of parts-per-trillion for compounds of science interest, which is extremely strict. Commercially available gases (MIL- PRF-2740 class C; 99.995% maximum purity for N_2) do not satisfy this requirement, even though the greatest fraction of the hydrocarbons present is C1-C3 volatiles, which will stay in the purge flow during integration and are not of concern with regards to contamination of any spacecraft surfaces. The probability of compounds of science interest remaining in a commercially available ultra-high purity purge gas is exceptionally low. To ensure that purge gas does meet requirements, off-the-shelf, point-of-use purifiers can be used. The semi-conductor and electronics industries have

driven the state-of-the-art in the gas purification and pure gas handling industry, such that parts-per-trillion point of use purification and analysis are common within that industry and readily available. Common techniques for the measurement of gas purity are incapable of measuring below the few parts per billion concentrations. However, commercially available specialty gas sampling systems are available for measuring gas purity down to the one part per trillion level. The purge gas cleanliness has been verified at approximately parts per trillion levels for both semi- and non-volatile hydrocarbons.

In the DRM concept, the purge flow passes through the sample collector geometry, out through the collector-cover labyrinth seal. With the addition of a barrier, the purge exhausted from the collector is available to fill a barrier's internal volume before exiting the barrier, thereby maintaining a positive pressure that protects the sensitive hardware surfaces from exposure to airborne hydrocarbons and bioburden.

Barrier Design Trades

Initial barrier concept designs underwent repeated iteration with design analyses (Barrier Conceptual Designs box in **Figure 2**). Three types of barriers were evaluated: 1) soft-sided bag with no structural support (non-rigid), 2) soft-sided with a skeletal support (semi-rigid) and 3) hard-sided (rigid). The barrier concept selected was a semi-rigid design because the non-rigid concept had poor structural integrity and the rigid concept had a high mass penalty. The non-rigid and rigid concepts were not studied in further detail. The soft-sided barrier with skeletal support and independent opening concept was developed leading to a one-third scale demonstration performed in the ILC Dover facility. Launch environmental conditions for the demonstrations were modeled rather than fully simulated.

Barrier Hardware Development

A soft-sided barrier naturally takes the shape of a cylinder on the sides and a dome on the end while under positive internal pressure relative to the barrier exterior. Positive internal pressure environment is unavoidable due to launch-ascent venting and contamination prevention measures. This barrier geometry limits the placement of spacecraft components, such as communication antenna, payloads, thrusters, and solar arrays that need to stay within the overall cylindrical spacecraft geometry and not prevent the required, nearly equal spacing of the skeletal rods that power the barrier deployment. Missions with RTGs installed present additional challenges due to the need to install RTGs exterior to the barrier, which further complicates barrier removal and RTG installation.

Spacecraft waste heat during launch integration and launch ascent are mission-specific considerations. Limiting the equipment that will be powered prior to launch will help decrease waste heat that must be removed from the within the barrier. If RTGs and a full spacecraft barrier are required of mission design, then RTG heat disposal needs to be addressed to mitigate thermal risks, especially if the clearance between the barrier and LV fairing is tight.

Contamination Transport Simulation Program Numerical Model

This study used the Contamination Transport Simulation Program (CTSP) contamination modeling software made available by Particle in Cell Consulting, LLC (Westlake Village, CA). Model validation was reported by Brieda (2018). The CTSP was modified by the vendor to incorporate the physical models and features needed for our study application and these revisions were incorporated in CTSP version 1.5. The modeling also included continuum flow models from CFD codes that simulate the convective and diffusive transport, chemical reactions and viscous effects in mixtures that were physical forces and dynamics to particles in a flow and sorption parameters for spacecraft surface and target molecules. Spacecraft and barrier dimensions entered as were incorporated through computer-aided design (CAD) models.

Model Framework

A summary of the new high-fidelity physics, contamination transport model is provided here, and details are given in **Supplementary Material**. In brief, inputs to the CTSP model were based on both molecular and particulate transport in terms of sinks and transport phenomena. Materials disperse from and accumulate in sinks. Sinks may: 1) trap a particle or molecule, 2) temporarily trap a molecule or particle, or 3) prevent further transport of a molecule to a sensitive surface (*e.g.,* blocking features like vents, labyrinths, filters, barriers, etc.). Sinks were addressed as additive collections. In contrast, transport was considered a fractional reduction process. During transport, the number of source particles or molecules that arrive at a contamination-sensitive surface is usually a fraction of those generated by the source due to the various sinks along the pathway. Differentiation of species and particles was expected due to the physics of the various sinks and transport phenomena. For molecular behavior, the model adopts the Brunauer, Emmett and Teller (BET) theory (Brunauer et al., 1938) for the equilibrium behavior of molecular adsorption on surfaces, which also applies to non-equilibrium conditions.

Spores and microbes, both viable and non-viable, are treated as a special case of particulates. Biological adaptations for surface attachment films, such as slimes, are ignored because bioburden reduction measures yield exceptionally low microbial populations on surfaces. If the microbes present were not physically or chemically bound to surfaces, the adhesion of the microbes to the surfaces was considered similar to non-biological particles. Low levels of microbes are expected in the LVE low biomass LVEs used for life-detection missions. Evidence of bacterial, archaea, and fungi, have been detected in the low biomass LVE were inventoried from witness foils collected during assembly, test, and launch operations for the OSIRIS-REx mission (Dworkin et al., 2018; Regberg et al., 2020).

Contamination transport was evaluated based on mission stages (launch processing, launch, cruise, operations) and transport processes and included: 1) verifying the efficacy of biomolecular barrier protection of the spacecraft, 2) determining the probability of the particle and molecular intrusion across the collector-cover labyrinth seal, 3) verifying the efficacy of an in-cruise collector bakeout, and 4) determining the probability of plume ice-particles transferring molecules, microbial material, and dust particulates to the instrument inlet.

Transport from the external barrier to the spacecraft was not modeled since particulate contamination is expected to be almost entirely retained on the barrier's exterior due to the extremely low acceleration forces on the barrier opening. Molecular transport is expected to be negligible, due to the very short exposure time and the narrow view of the barrier's external surface to the spacecraft during and after opening. In both cases, the velocity vectors of the contamination from the exterior of the barrier point away from the spacecraft. Similarly, transfer from the collector cover's exterior to the collector was not modeled for the same reasons.

In adopting the refined contamination engineering approach discussed in *Contamination Control Engineering Principles*, the modeling effort traced backward from the instrument inlet (defined as the end of the contamination transport pathway) through the various paths to the fairing and launch environment, describing the sinks and the interfaces. It was assumed that the instruments have met all their performance and cleanliness requirements and that transport in the instrument payload is lossless until it is in operation. The time frame for the modeling process starts with delivery for encapsulation into the fairing and ends with sample collection for science operations.

Particulate Transport

The greatest concern for particle contamination the spacecraft is transport from the LV's fairing during launch. During a normal launch, the acoustic vibration and acceleration of the LV and coupled loads result in the detachment of particles, driven by a complex function of forces including particulate adhesive detachment, and acceleration forces as well as entrainment of particles in the high-velocity vented air flow. Considerations for these forces are described in **Supplementary Material**.

This study assumed that the fairing meets the existing NASA cleanliness requirements for current less sensitive science missions. During launch with a barrier-contained spacecraft, the contamination-sensitive spacecraft surfaces are protected. The barrier being much smaller than the faring, specifically designed for low outgassing, and precision cleaned, provides a significantly cleaner environment than the fairing. Adding a barrier to the spacecraft payload eliminates the necessity for costly and potentially risky changes to the fairing design and processing—such as requalification of the fairing; changing materials; developing new fabrication, bioburden reduction and/or cleaning processes; changing launch processing flows; and updating launch facilities. This approach can benefit other ultra-sensitive missions by isolating the payload from the LV. It may also avoid the cost of making the newer commercial LVs compatible with missions that are contamination sensitive albeit less than that for a life-detection mission.

Molecular Transport

The transfer of organic chemical or other molecular contaminants to the inlet of instrument systems occurred by

two primary modes: 1) gas-phase transport during launch and cruise, and 2) contact-driven transport during sample collection, which for the DRM involves the Enceladus plume ice particles hitting possible contaminants on the sample collector surface, releasing them for transport. In the DRM, >90% of ice particles entering the collector transport to the instrument inlet (Willson et al., 2017). The model assumed that the molecular contamination was primarily present as a discrete monolayer of molecules adsorbed directly on the collector's surface (**Figure 1**). The transport was probabilistic, based upon the limited number of particles expected. If the energy imparted by a particle impact exceeded the surface adsorption energy, then the molecule would be removed. Gas-phase transport follows standard statistical emission, line-of-sight transport, and adsorption behaviors. Gas-phase transport is also highly temperature dependent. Molecular contamination can transport by evaporation and redeposition and its transport rate is exponentially related to temperature, based upon the Arrhenius relation. Molecular evolution from a surface is described as occurring in a Lambertian distribution. The molecular flux is described as a cosine distribution from the surface normal. Both relations are simplifying assumptions.

Modeling of evaporative transport mechanism was carried out utilizing a particle-in-cell technique (Brieda, 2018) dividing the collector geometry into discrete mesh elements. Exemplary molecular species were allowed to evaporate, transport, and redeposit based upon their physical and chemical properties. The classical approach for addressing the adsorption and desorption of molecules from surfaces assumes that there is a single enthalpy of adsorption for all species from all surfaces. In our modeling, we chose four distinct molecular species having distinctly different enthalpies, to better address the transport differences. In addition, as stated in Brunauer et al. (1938) at the monolayer and sub-monolayer level of molecular coverage, the enthalpy of adsorption for a species can be estimated as the enthalpy of sublimation for the species, which was incorporated into the sorption modeling to address greater enthalpy of adsorption associated with monolayer and sub-monolayers. To incorporate properties of the materials adsorbed on bare surfaces into the modeling code, it was necessary to incorporate a material-material interaction. CTSP treats molecules as particles having specific molecular properties. As a CTSP particle interacts with the surface of another material, whether it be a bare surface or a surface covered with molecules of a defined type, the enthalpy of sorption defines the material-material interaction. Incorporating enthalpies of sorption for select molecular species allows more realistic modeling of the molecular interactions with specific spacecraft surfaces, leading to a more physically correlated interaction. Description of the incorporation of this material interaction is described in the CTSP users guide[3] for the CTSP version 1.5. In the implementation for this work,

enthalpies of sublimation were used to approximate the sorption properties of molecules at the monolayer and lower coverage levels.

Model of Collector-Cover Labyrinth Seal
In the DRM, the cover of the collector provides primary protection preserving the cleanliness of the collector from payload integration, throughout the assembly, test, launch operations, and cruise, until the cover is removed when the probability of new contamination from the external environment is exceptionally low. Instead of using an overpressure for evaluating of the required purge gas flow, we used the CFD in the model to determine the required mass flow of purge gas to prevent intrusion of molecular contamination by back diffusion through the labyrinth seal. The flow across the collector-cover labyrinth seal is a function of seal geometry, purge gas composition, and flow velocity. These three factors impact the conductance of materials in the opposite direction of the venting gas flow. The labyrinth seal geometry was designed based upon heritage designs. The purge gas composition was chosen to be nitrogen due to the broad availability and ease of purification. Given the fixed geometry and the selected purge gas, the purge gas flow rate was left as the independent variable for assessing the efficacy of the purge within the designed system. In the laminar flow regime, flow velocity is not constant across the gap in the labyrinth seal; instead, flow is zero at the wall and increases toward the center of the labyrinth seal gap.

The flow profile was modeled to ascertain the rate of contamination transport into a volume. The simulated over pressure for the purges through the labyrinth seal from the inner boundary region to the outer boundary region was up to 3 Pa. This is largely due to the geometry of the labyrinth seal; a less tortuous path would require higher over pressure and flow for an equivalent efficacy. For particle transport, the resolution of the flow profile was that of the particle size. Evaluation of the efficacy of the collector-cover labyrinth seal in preventing particle infiltration into the collector assembly was initially conducted without a purge using CTSP. This evaluation utilized 10 million simulation particles representing a level 100 particle size distribution (2.19×10^{-4} percent area coverage). For molecular transport, flow profile was evaluated with purge at a higher degree of resolution to capture the complex, non-linear behavior of molecular diffusion. More detail concerning the evaluation of the purge is in the supplement.

Model of Launch Environment With and Without a Barrier
The particle fallout due to launch was evaluated using the standard ULA fairing cleanliness and conditions outlined in the Atlas V Launch Services User's Guide March 2010 and assumed to be representative of cleanliness conditions of fairings by other LVPs. The airflow through the fairing was modeled using CFD and assuming the vibration and acceleration profiles inside an ATLAS V 5-m long fairing. The assumption of a level 100 spacecraft surface (*i.e.,* 2.19×10^{-4} percent area coverage (PAC) based upon IEST-STD-1246) was made in both the barrier and the no barrier cases. In the

---

[3]https://www.particleincell.com/files/papers/CTSP-UG.pdf.

barrier case, level 100 was also assumed for the barrier. The particle cleanliness of the ATLAS V 5-m fairing was defined as level 500, which is consistent with the specification level for the inside of the fairing. Venting airflow was computed accounting for the fairing venting. The flow in the barrier is defined by the depressurization of the barrier through the vent valves in the barrier, with respect to the pressure in the fairing. The efficacy of the barrier purge for molecular contamination intrusion was determined by using CFD. Purge flow rate was too low under static conditions to dislodge particles, therefore CFD modeling of particle transport was only carried out for ascent venting. The launch profile was the same as for the barrier and no barrier cases.

More specifically, continuum flow inside the LV fairing and spacecraft barrier was simulated using the Mississippi State University CFD solver Loci/CHEM version 4.0. The 3D Reynolds-averaged Navier–Stokes (RANS) equations were solved neglecting the turbulence effects and using the Chorin-Turkel local preconditioning scheme for the inviscid terms. The time integration was accomplished by a robust second-order accurate three-point backward time scheme. The binary mixture (i.e., air inside the fairing and purge N_2 gas) was modeled as made of inert gases. Finally, the solid walls implemented a second-order, characteristic-based, slip-wall boundary condition. Fairing vents and seal gap used a transient outflow and fixed mass-flow-rate inflow boundary conditions, respectively. The time history for the static pressure at the fairing vents adopted the venting analysis published in the LV user manual.

Model of the In-Cruise Collector Bakeout Activity

The collector for plume sample in the DRM is the largest of the critical surfaces that samples are exposed. Based on the above modeling verifications, it is expected that the collector, which was 1) precision cleaned to level 100 or better, 2) been isolated by the cover with labyrinth seal for launch operations and most of the cruise duration, and 3) protected by the barrier and purge during launch operations, has preserved its level-100 cleanliness. Still, given the stringent contamination requirements, an extra procedure was considered to ensure its cleanliness prior to sample collection. A bakeout of the collector surface in the vacuum of space at >250°C for 60 min with the cover removed was a feasible choice in the DRM scenario.

To evaluate the efficacy of the in-cruise collector bakeout procedure, molecular emission was modeled for a bakeout at 300°C for 60 min starting with an unrealistic ubiquitous monolayer of contaminants having physical and chemical properties (i.e, range in volatility and adsorption energy) aligned with lipid-hydrocarbon target compounds listed in L1 science requirements from the DRM (e.g., carboxylic acids). The molecules selected for molecular transport modeling of the collector included n-dioctyl phthalate, n-hexadecane, n-eicosane, and n-pentacosane, which are conservative for space hardware that has gone through component-level, thermal-vacuum bakeout prior to payload and spacecraft integrations. Amino acid target compounds or their associated

biopolymers (peptide and proteins) were not included since high temperatures are known to degrade them (*Target Compounds*). In reality, the molecular level would be less than a monolayer and composed of a variety of non-volatile materials. However, the simplified modeling conditions allow for verification and an understanding of the emission process.

The rate of evolution (τ_{res}) was modeled using a surface residence time calculation expressed as,

$$\tau_{res} = \tau_0 e^{\left(\frac{\Delta H_{vap}}{RT}\right)} \qquad (1)$$

where τ_0 is the molecular vibration period, ΔH_{vap} is the enthalpy of vaporization for the molecular species, R is the gas constant, and T is temperature in Kelvin. The solution was scaled to the surface area covered by molecules of the same type, at the same evaporation enthalpy.

Model of Contamination Transport by Plume-Ice Impact

Given the impingement of plume ice particles on the collector surface, surface contaminants may be transferred to the instrument inlet at the base of the collector. The probability of contaminant transfer is a function of the amount of energy deposited per unit area at the collector surface by the ice particles and whether the point of impact contains a contaminant. It was assumed that if there was sufficient energy density to remove a contaminant, but there no contaminant was present, then there was no contamination transfer. Estimates of the number and area of impact events per particle size, supported assessment of the energy dissipated in these events, the energy required to dislodge potential contaminants, and the cross-sectional area of the contaminants on the collector, and the quantity of material delivered to instrument inlet. By determining the fraction of the contaminants transferred, the allowable quantity of individual contaminants on the collector surface can be determined.

Particle-size distribution of the Enceladus plumes comes from Cassini mission results. Ice particle mass and density, which influence particle dynamics, were calculate based on formation processes described by Steddum (1971). Both are described in detail in the **Supplementary Material**. Assuming ice-particle size distribution and 50 μL of plume ice impacting the collector, the number of ice particles of each size was calculated. For each type of potential contaminant in the collector, the energy required for removing the contaminant from the surface of the collector was then calculated.

Ice-Driven Molecular Contaminant Transport

In the case of molecular transport driven by ice impact, it was assumed that the molecular contamination would primarily be present as a uniform monolayer of molecules adsorbed directly on the collector (*Model of the In-Cruise Collector Bakeout Activity*). Conversion of this base case to other cases only requires scaling to the fractional area coverage of different species. The transport was probabilistic. It was assumed that the energy required to remove the molecules from the surface
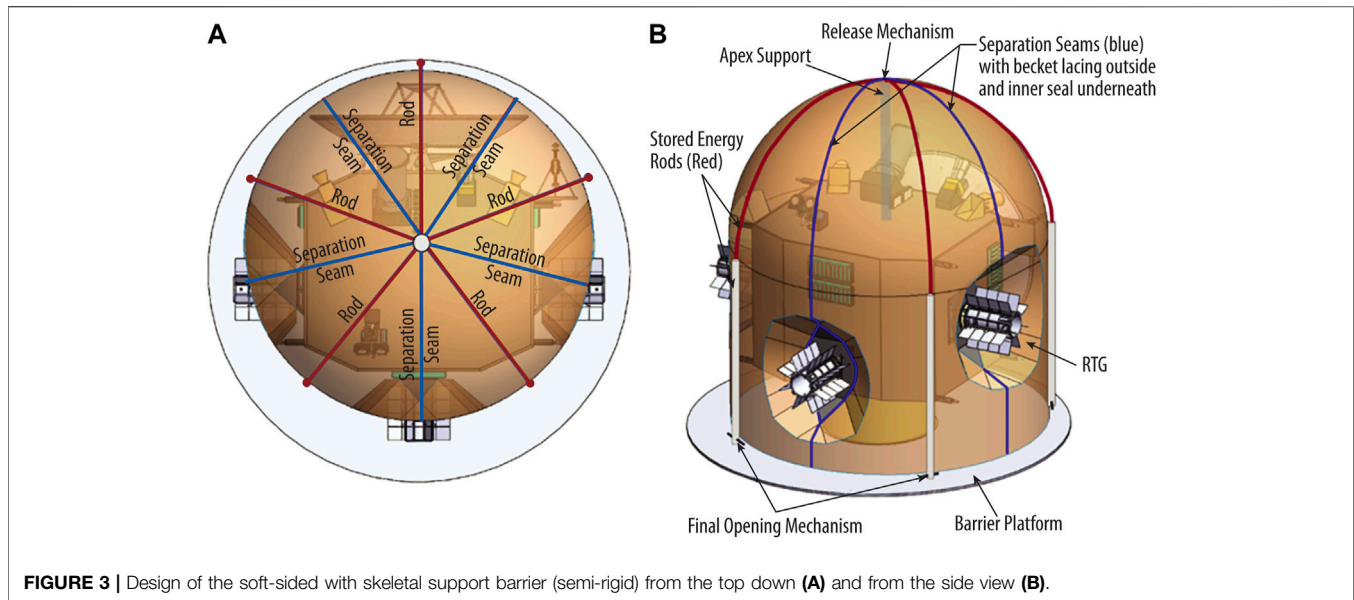
FIGURE 3 | Design of the soft-sided with skeletal support barrier (semi-rigid) from the top down **(A)** and from the side view **(B)**.

would be due to the surface adsorption energy. Thus, if the energy imparted by the particle to the adsorbed molecule were less than the surface adsorption energy the molecule would not move. If the energy imparted by the particle exceeds the surface adsorption energy, then the molecule would be removed.

Ice-Driven Dust and Microbial Particulate Contaminant Transport

Plume-ice-particle driven transport for particulate contaminants on the collector surface was evaluated based upon the incident ice-particle energy and the impacted collector cross sectional area, assuming strong adhesion to the surface and other factors (**Supplementary Material**).

The tensile strength of ice (1×10^6 N/m^2), the relative elongation to failure of 0.01%, and a nominal ice-bond thickness, were used to calculate the resultant energy required to displace particulate contaminants (**Supplementary Material**). To determine the probability that a particulate contaminant entering the instrument inlet at the base of the collector, initial assumptions on particle distribution were made. For dust particles, a starting point of level 100 cleanliness or better, the number of particles at or above 1 μm per 0.1 m^2 is 5,058 or less. For bioburden related particle distribution, a nominal viable bioburden level of 300 colony-forming units per m^2 and the assumption that they are 1% of the total burden of viable and non-viable microbes, there would be 30,000 microbes per m^2, each microbe being assumed to be a 1 μm-diameter sphere with a cross-section ~3.14×10^{-12} m^2.

RESULTS

Barrier Design

The resulting barrier design is described here in brief. Details are provided in the **Supplementary Material**. This semi-rigid barrier

is attached to the launch vehicle below the spacecraft separation plane and consists of a mostly free-standing light weight structure with stored energy rods and a final opening release mechanism. When the mechanism is activated, the energy stored in the skeletal rods provide the force required to open the barrier fully, thereby allowing the spacecraft to be separated from it and the LV. The resting position of the rods allows plenty of clearance from the spacecraft during its ejection from within the barrier. A structural support between the top of the spacecraft and the barrier apex provides stability in the launch environment. A barrier platform attached to the LV is also required to integrate the stored energy rods as well as other equipment like vents. The barrier skin is a dual-layer material divided into 4 to 6 panels that are attached to the lightweight structure at the middle of each panel with seams between each of the panels that span from the base to the apex (**Figure 3**). The outer layer provides the structural support for the high tensile load experienced during launch ascent and the inner layer provides the contamination protection function.

The outer layer material is connected at seams in a manner that is high strength while permitting unencumbered separation. Kevlar was identified as a possible outer layer material. The outer layer must minimize or eliminate all loads that could damage the contamination prevention inner layer seal. Ideally, the inner layer should be integrated with the outer layer, for simplicity of operation, except at the seams which need to be separate. A candidate integrated flight material is a thin Kapton inner layer bonded to a Kevlar outer layer; however, there are strength, flexibility, porosity, thermal expansion, material bond ability, outgassing and other requirements that will affect the final material choice. An existing fabric with a Vectran outer layer bonded to a Mylar inner layer should meet the design requirements, but it has not been fully qualified.

The design of the seams between the barrier panels is one of the most critical elements of the barrier. The seam must
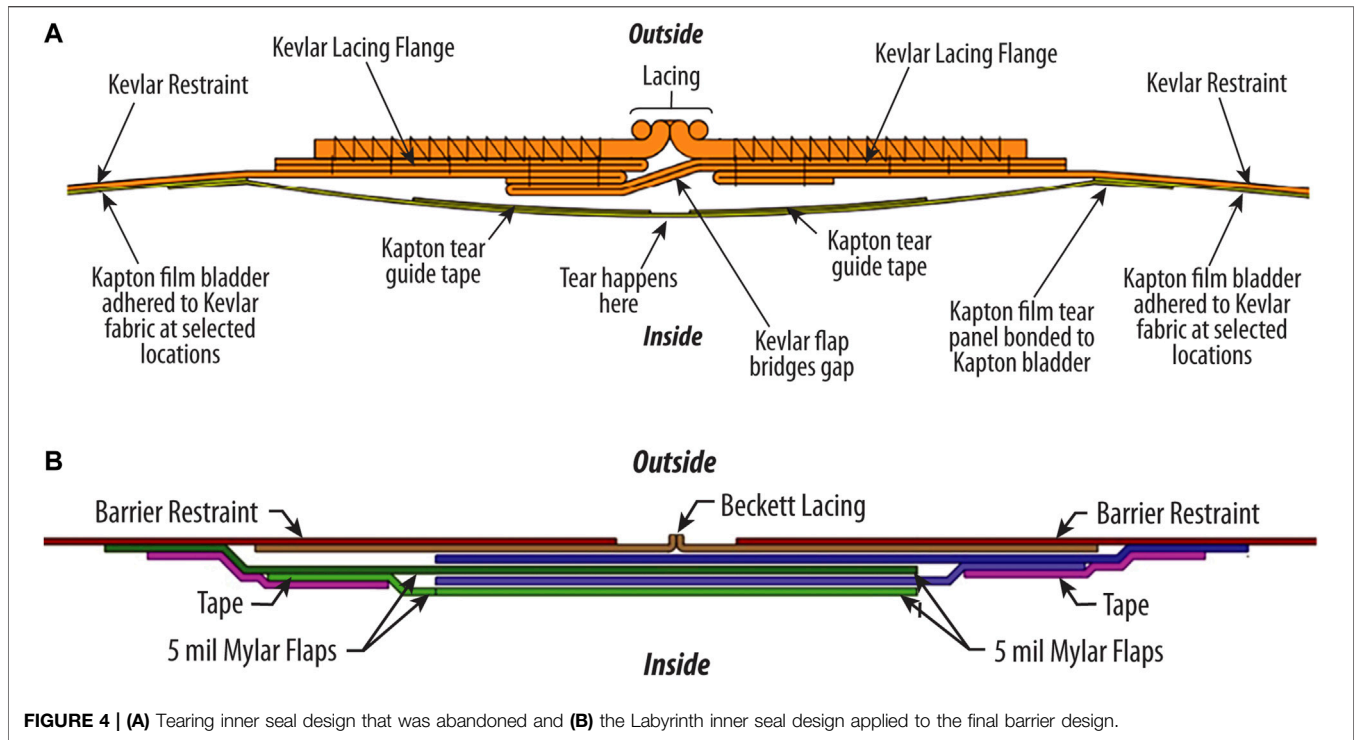
FIGURE 4 | (A) Tearing inner seal design that was abandoned and **(B)** the Labyrinth inner seal design applied to the final barrier design.

TABLE 2 | Barrier mass estimate.

Description	Unit CBEMass (kg)	Qty.	Total CBE Mass (kg)	Cont.	Total MEV Mass (kg)	Assumptions
Soft Goods	19.0	1	19.0	25%	23.8	Subtracted RTG Barrier support plate
Barrier Platform	13.6	1	13.6	25%	17.0	Al honeycomb (2.1 lb.ft^3; 0.13 kg/m^3) Al face sheet thickness is 0.015-inch, total thickness is 1.0-inch
Platform Structure	5.0	1	5.0	25%	6.3	rough estimate
LV Separation Area Barrier Structure	2.0	1	2.0	25%	2.5	rough estimate
Vents in Platform	2.0	2	4.0	25%	5.0	rough estimate
Apex Support	2.5	1	2.5	25%	3.1	Carbon Fiber Tube: outer diameter is 3.0-inch, wall thickness is 0.125 inch; mounting bracket is 1.4 kg (rough estimate)
Stored-Energy Rods	0.6	5	3.0	25%	3.8	Tapered Carbon Fiber Tube: outer diameter #1 is 1.0-inch, outer diameter #2 is 0.25-inch, wall thickness is 0.063-inch, length is 175 iinch
Final Opening Mech	2.5	5	12.5	25%	15.6	Estimate from current design
Release Mechanism	0.5	1	0.5	25%	0.6	Estimate from current design
RTG Barrier Support	1.0	3	3.0	25%	3.8	3 RTGs installed
Total Mass (kg)			65.1		81.4	
Mass (lbs)			143.2		179.0	

withstand high tensile loads, prevent contaminants from entering the barrier, minimize the leakage, and easily open upon command. The employed strategy is to incorporate an outer structural seam and an inner non-structural sealing seam. The selected outer structural seam is held together by a becket lace made of Kevlar braid that will unzip when the top lace is released, and sufficient force is applied to pull open the seam (**Figure 4**). Two inner seam designs were evaluated: 1) Kapton tear seal, and 2) labyrinth Kapton seal. The first concept, most desirable from a

sealing capability, bridges across the Kevlar braid. The idea is the thin Kapton will tear predictably if guided, when the becket lace is released, from the force generated by the stored-energy rods (**Figure 4A**). This concept worked for straight trajectories but did had problems when the tear trajectory changed in 3 dimensions. This design concept was abandoned for this study but with additional evaluation may be able to achieve success. The second inner seal design eliminates the need to tear the sealing seam by incorporating a labyrinth seal (**Figure 4B**). The labyrinth
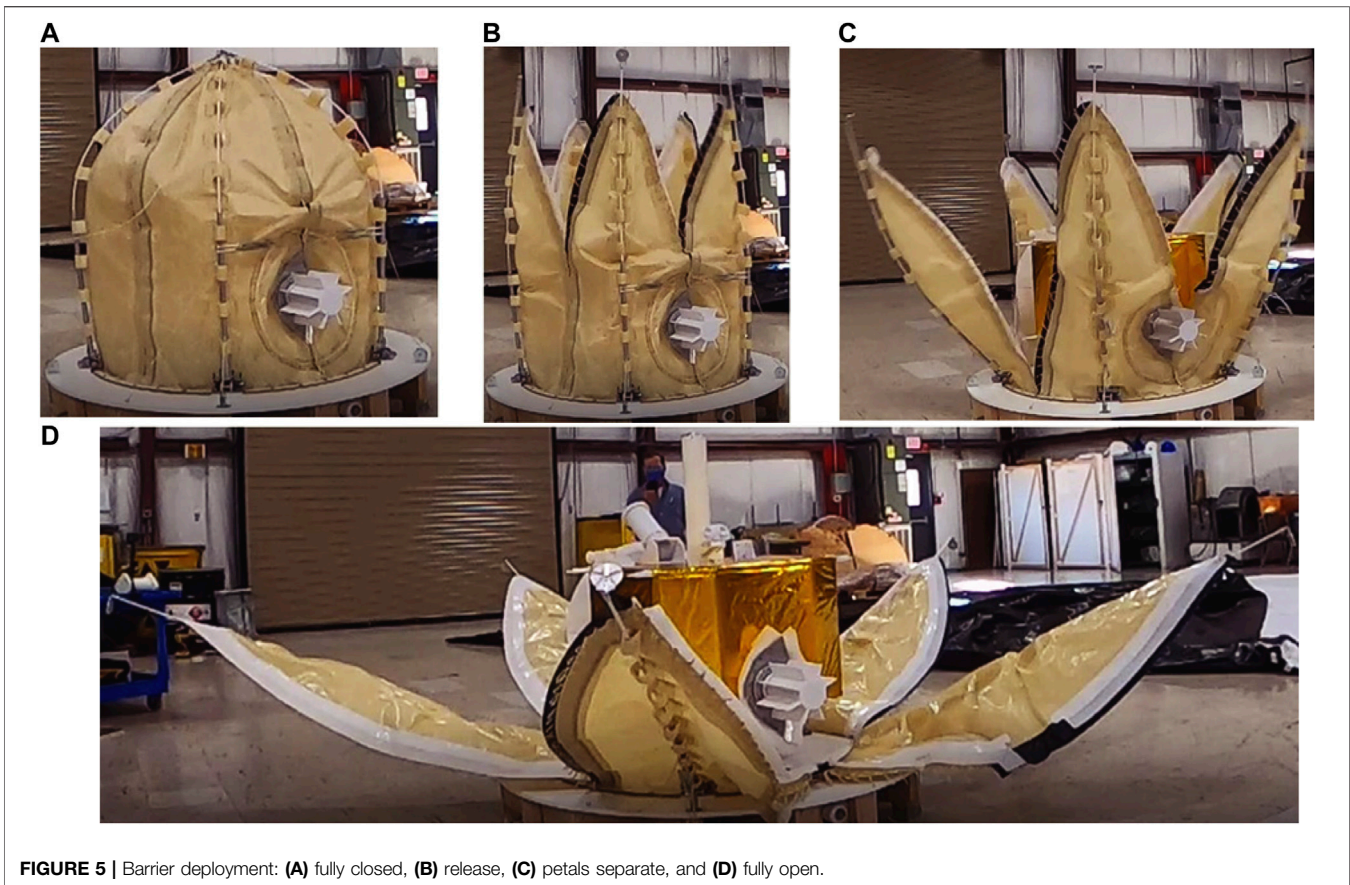
FIGURE 5 | Barrier deployment: **(A)** fully closed, **(B)** release, **(C)** petals separate, and **(D)** fully open.

seal has interleaving layers of Kapton, creating a tortuous path for contamination to pass. When the becket lace is released, the layers slip apart allowing the barrier to fully open. The primary disadvantage of the labyrinth seal is that since it is not a single continuous layer, it is likely to present some leakage. Increasing the required flow rate of clean purge gas will maintain a positive pressure in the barrier.

The mass of the barrier for the DRM with a volume of 21 m^3 is provided in **Table 2**, however, barrier mass is directly linked to the size of the spacecraft, so any mass estimate for other missions will need to be scaled. There is also uncertainty in the total mass because some barrier elements were not evaluated in detail, such as the platform, vents, apex support and platform support structure.

The barrier's design is a simple geometry, which supports precision cleaning with standard solvent, peroxide, or DHMR processes that reduce bioburden and contaminants. The materials are also non-particle shedding, which significantly decreases the total number of particles transferred to the spacecraft by reducing the total contaminant load exposed to the spacecraft.
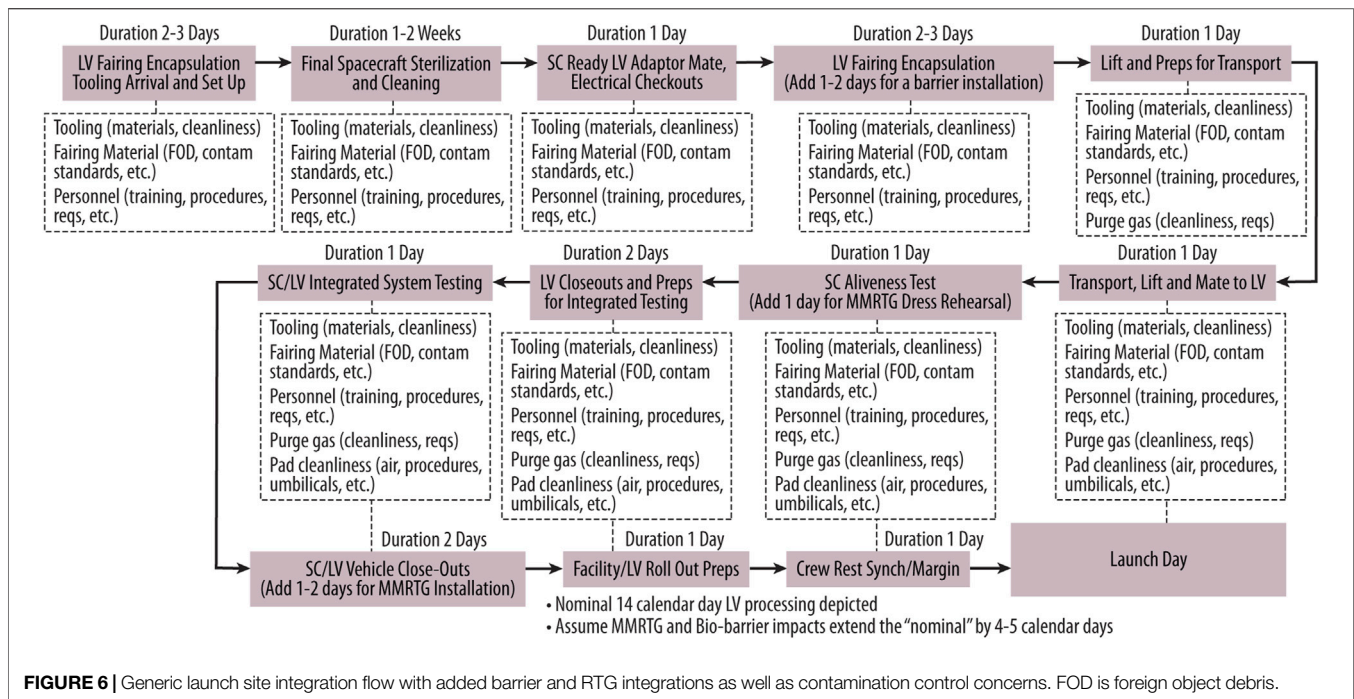
Barrier Deployment Demonstration

The successful build and deployment of the 1/3-scale barrier prototype around a spacecraft mock-up complete with a single RTG demonstrated the barrier functionality. For simplicity, a spacecraft mockup with a single RTG was demonstrated, but the

design principles apply to spacecraft with multiple RTGs. The demonstration barrier contained all the major elements identified for the barrier. These included: 1) Outer structural layer/seal and inner labyrinth contamination prevention layer/seal; 2) Stored-energy rods that provided the force required to fully open the barrier, 3) Platform structure, and 4) Single action deployment mechanism. Some elements of the demonstration model, such as the release mechanism and the skeletal stored-energy rods, were simplified for ease of construction. Differences between the demonstration unit and the flight design are detailed in the **Supplementary Material**. The barrier opening event completed in less than 1 s plus up to 10 s for motion to be damped. **Figure 5** shows the deployment sequence from the demonstration. Videos and more images of the demonstration are available in the **Supplementary Material**.

Barrier Purge Gas

The barrier will be constructed with an absolute minimum of outgassing materials, cleaned to a high level and bioburden reduced prior to installation and will be purged up to launch. The interior of the barrier is expected to have a minimal amount of non-volatile residue. At launch, the barrier will have some level of overpressure, nominally less than 0.1 psi. The viscous flow regime slows the redistribution of non-volatile residue. This overpressure will be maintained by a vent/pressure relief valve, preventing the barrier from reaching too high of a differential

FIGURE 6 | Generic launch site integration flow with added barrier and RTG integrations as well as contamination control concerns. FOD is foreign object debris.

pressure versus the environment. The pressure relief will also maintain sufficient pressure to maintain viscous flow until the opening of the barrier.

The purge flow into the barrier will flow out of the sample collector through a labyrinth seal into the barrier protecting the sensitive hardware surfaces. The purge maintains positive clean gas flow out of the cleanest hardware to areas with lower sensitivity to hardware cleanliness. The purge will establish a flow profile that contaminants must overcome to enter the most critical hardware. Upon launch, the gas flow into the purge system will cease. During ascent, the pressure outside of the barrier will decrease and the gas in the barrier will begin venting. There will be a net flow out of the collector as the pressure in the barrier decreases. Due to the flow restriction of the labyrinth seal, flow will continue for some duration on ascent. This will decrease the opportunity for materials on the spacecraft to enter the sample collector.

The flow and depressurization control will limit the redistribution of molecules due to the limited time between purge cessation and barrier ejection. With the maintenance of pressure in the barrier, the gas flow will be within the viscous flow regime. This will result in the limitation of the evolution of the molecular contamination to the molecular diffusion regime. The evolution of molecules from a surface will create a local concentration gradient; this decreases the effective rate of evolution of contaminants from a surface. This is due to the local increase in the concentration at the surface thus reducing the potential gradient.
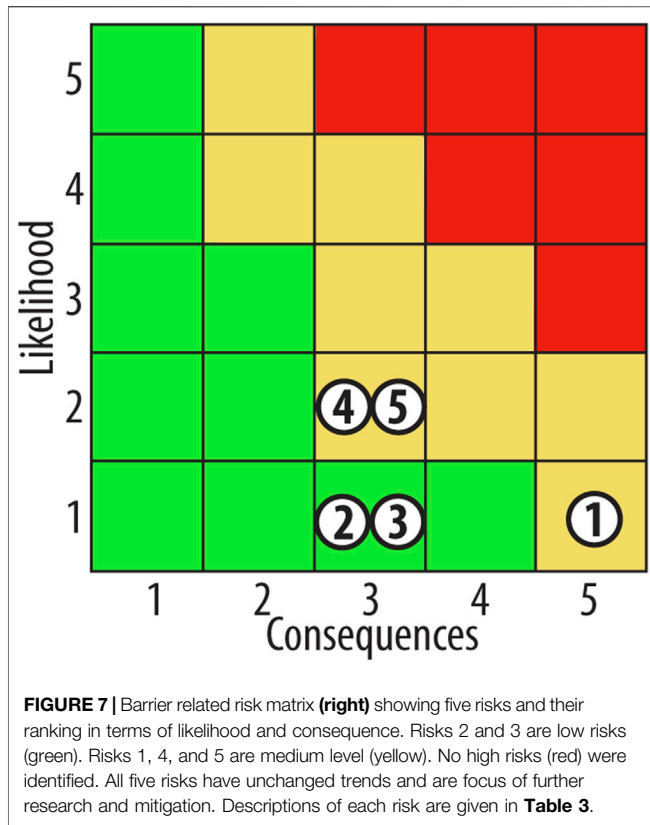
Contamination accumulation on the launch pad will be a function of the internal contamination level on the inside of the barrier and the efficacy of the purge. The efficacy of the purge is a function of the cleanliness and the properties of the purge gas, the

purge gas flow rate, and the flow characteristics of the labyrinth seal and the concentration and transport properties of the contaminants.

Barrier Integration and Operation

Construction and launch site integration will require additional cleaning and decontamination steps (**Figure 6**). Spacecraft for life-detection missions will undergo extreme efforts in parts selection and cleaning at all stages of construction. These may include selection of parts with extremely low outgassing, sterilization of subsystem boxes by chemical or thermal means and the inclusion of HEPA filters on all venting ports. Final processing of the spacecraft at the launch site will likely be done in an extremely clean tent (ISO class 5, equivalent to FED STD Class 100). Any component above the base of the barrier will have to be precision cleaned before being integrated. For example, the spacecraft half of the LV adaptor will need this sterilization and cleaning before attachment of the barrier base plate. Final spacecraft cleaning may require an extended duration of several days up to several weeks and various decontamination methods (heat, chemical vapors, solvents, wipes, and confirmation tests). At this time, the spacecraft is as clean as it will ever be, and the function of the barrier will be to minimize any additional contaminants. The barrier will have been precision cleaned and sterilized following manufacture and double bagged for transport to the launch site.

The barrier would be installed while in the very clean environment (following the second box in sequence of **Figure 6**). The most sensitive components of the spacecraft science payload will have been sealed tight or kept under continuous purge with ultra-pure gas. For the DRM, cleanliness preservation methods for the payload are for

FIGURE 7 | Barrier related risk matrix **(right)** showing five risks and their ranking in terms of likelihood and consequence. Risks 2 and 3 are low risks (green). Risks 1, 4, and 5 are medium level (yellow). No high risks (red) were identified. All five risks have unchanged trends and are focus of further research and mitigation. Descriptions of each risk are given in **Table 3**.

instruments and collector, respectively. After barrier installation, the collector purge and possibly additional barrier purge inlets will complete the inflation of the barrier by the purge gas and maintain a small positive pressure relative to the ambient atmosphere. This purge would continue until time of launch at T_0.

After barrier installation, LV fairing encapsulation can proceed along the standard integration flow (following the fourth box in the sequence of **Figure 6**). During this time the purge system must also have a feedback system that continuously senses changes in the ambient pressure, such as during LV fairing encapsulation and final testing. The feedback system controls the purge gas supply to ensure that a positive pressure is always maintained inside the barrier. RTG installation occurs approximately 3 days before the opening of the launch window and is a critical operation as the RTGs need to bolt through the special panels on the barrier. These lenticular shaped panels will stay with the spacecraft after barrier opening.

At launch (T_0), the purge gas feed to the barrier will cease. The ambient pressure outside the barrier will decrease to essentially zero over about the first 2 minutes of flight. Large vents in the barrier base plate must open sufficiently to let the large gas volume inside the barrier escape at a controlled rate to ensure that the differential pressure from inside the barrier to the exterior does not exceed the allowable maximum. At a predetermined time and altitude after the fairing is jettisoned, the barrier opening will be initiated by a timer. A cable cutter or pin puller will fire and release the clamps at the barrier apex. At

this point the seam support lacing will open, powered by the stored energy in the composite rods that support the barrier. Once the structural constraint of the lacing has been removed, the controlled weak lines of the seams between the barrier panels will tear, or slide open if it is a labyrinth, as the barrier petals open like a flower. After all the barrier petals have pulled away from the spacecraft, the Marmon clamp holding the spacecraft to the LV upper stage will release and the exceptionally clean spacecraft will be ejected to continue its cruise to the mission target.

With the barrier open, the spacecraft is exposed to the surrounding space environment at an altitude over several hundred kilometers. At this altitude, the environment is at vacuum with no risk of environmental contamination.

Barrier Risks

Risk analysis for the barrier was conducted to ascertain the validity of an identified risk, likelihood of that risk occurring, magnitude of the consequence of such an event, and timing for mitigating the risk. **Figure 7** displays the barrier related risk matrix and details of the risk details are described in **Table 3**.

Model Results
Probability of the Contaminant Intrusion Across the Collector-Cover Labyrinth Seal
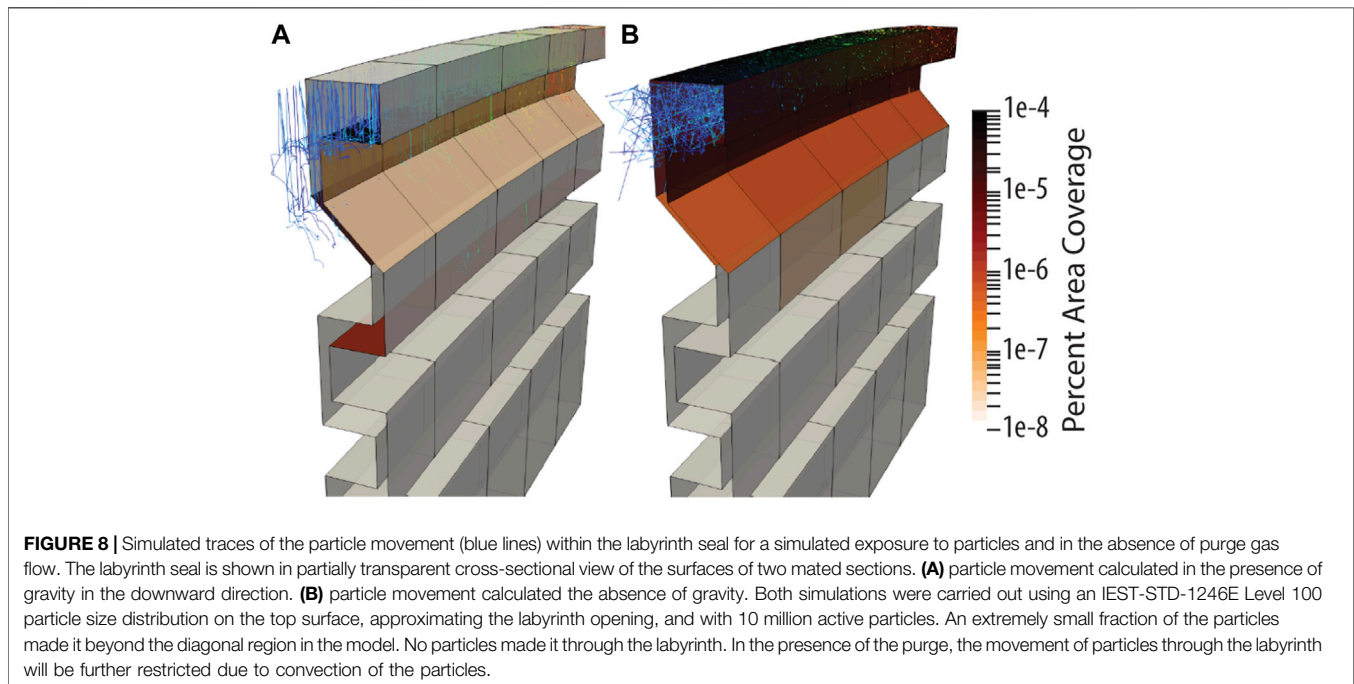
Model investigation of particle intrusion across the collector-cover labyrinth seal started with particles placed at the upper edge of the outermost groove of the labyrinth. Two simulations were carried out without purge, one accounting for gravity, and one without gravity (**Figure 8**). Simulations indicate that less than one of the 10 million particles infiltrated further than the first labyrinth section (diagonal portion), thus verifying the efficacy of the labyrinth seal for protecting the collector from contaminants from the external environment. Adding a purge to the collector, which would further impede possible intrusions from outside the collector and cover would further reduce the probability.

Molecular intrusion was investigated by close examination of the flow across the most restrictive part of the seal (diagonal section; **Supplementary Material**). Results show that the seal provides a high level of isolation of molecular contaminant diffusion, even when an extremely high external molecular contamination fraction was applied in the model. A more realistic case involves very low contamination fraction due to low outgassing materials for the barrier construction, which contributes further reduction of intrusion. Modeling the particle intrusion across the seal with a purge active was not pursued since the non-purge case demonstrated the seal was sufficient at protecting the collector surfaces from exterior contaminants. However, in the DRM scenario, purge of the collector, with flow from inside to outside across the labyrinth seal (opposite that in the model) and then into the barrier where it is then purged to the exterior, adds an addition level of protection for the collector that effectively eliminates contaminant intrusion while the purge is active. Details of the model results are provided in detail in the **Supplemental Materials**.

Modeling the convection-diffusion phenomena through the entire labyrinth seal was computational infeasible, thus the focus

TABLE 3 | Barrier related Risks.

ID	Risk statement
1	Given that the barrier depends on a mechanism to deploy There is a possibility that: the deployment mechanism will malfunction and not be released resulting in loss of mission science
2	Given that there will be excessive positive pressure differential between the inside of the barrier and the LV fairing There is a possibility that: barrier skin will be damaged resulting in payload contamination
3	Given that excessive negative pressure differential between the inside of the barrier and the LV fairing. There is a possibility that: the barrier skin will touch the spacecraft and possibly damage some spacecraft components resulting in spacecraft component damage and/or contamination
4	Given that there will be negative pressure inside barrier relative to outside of barrier There is a possibility that: spacecraft will be exposed to contamination resulting in requiring the spacecraft to be cleaned again
5	Given that the barrier is delicate. There is a possibility that: damage could occur to during handling resulting in contamination exposal and requiring the spacecraft to be cleaned again

FIGURE 8 | Simulated traces of the particle movement (blue lines) within the labyrinth seal for a simulated exposure to particles and in the absence of purge gas flow. The labyrinth seal is shown in partially transparent cross-sectional view of the surfaces of two mated sections. **(A)** particle movement calculated in the presence of gravity in the downward direction. **(B)** particle movement calculated the absence of gravity. Both simulations were carried out using an IEST-STD-1246E Level 100 particle size distribution on the top surface, approximating the labyrinth opening, and with 10 million active particles. An extremely small fraction of the particles made it beyond the diagonal region in the model. No particles made it through the labyrinth. In the presence of the purge, the movement of particles through the labyrinth will be further restricted due to convection of the particles.

of molecular intrusion was placed on the highest velocity region of the seal's gap. Even when an extremely high external molecular contamination fraction was used as an initial condition, the labyrinth seal provided a high level of isolation. In the case of the very low molecular contamination of the barrier internal environment, the transport across the seal into the collector would be even lower.

Model Verification of Barrier Efficacy

Efficacy of the barrier was demonstrated by comparison to a spacecraft open to the fairing environment. Model results show the flow velocities within the fairing for the no barrier and barrier cases, as well as within the barrier (**Figure 9**). During the ascent, particles from the larger area fairing are dislodged and entrained in the exhausting airflow from the fairing. In the no barrier case, fairing particles fell and stayed on the spacecraft during ascent resulting in a significant increase in the number of particles on the top deck of the spacecraft (**Figure 10A**). For the same initial particle loading, the

barrier was shown to isolate the spacecraft, minus the unprotected RTGs, from the flow of fairing particles resulting in a significant decrease the particulate load on the spacecraft (**Figure 10B**). For particles, the isolation is greater than one in ten million. For molecular contaminants of concern, no molecular intrusion was predicted under very conservative conditions.

Based on model results for launch and assuming less energetic conditions of pre-launch activities, it is expected that the barrier would provide effective isolation from the exterior environment for all pre-launch activities. The barrier effectively isolates the spacecraft from the intrusion of exterior contaminants once installed and purge activated.

Decontamination Efficacy of an In-Cruise Collector Bakeout

Modeling of the collector bakeout showed that as the surface became depleted in contaminants through evaporative loss, or
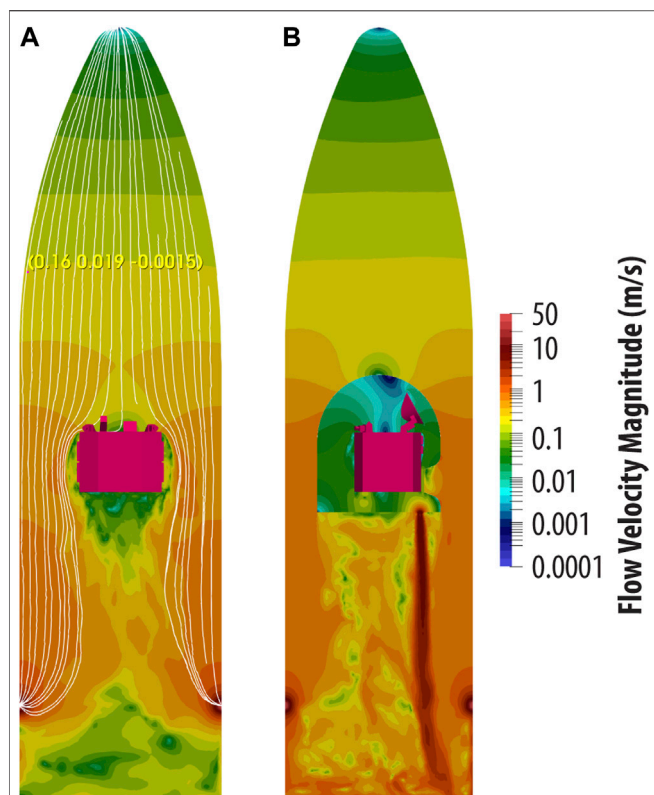
FIGURE 9 | Direct comparison of rendered flow velocity magnitudes at 100 seconds into launch without a barrier **(A)** and with the barrier **(B)**. The two images are slices of the computed three-dimensional flow profiles at similar depths into the fairing and at the same time into the launch. Streamlines for the flow of air out of the fairing through the fairing vents are show in **(A)**, but were removed from B for visual simplification. Based on the geometry of the LV, spacecraft, and the bio-molecular barrier [for **(B)** only], the flow is primarily cylindrically symmetric. Particle transport simulations addressed fluid dynamics in three spatial dimensions over time and associated with LV acceleration, all of which impact the particle redistributions.

coverage increased due to adsorption, the fractional area coverage changed. An average of 12.9% of the exemplary contaminants remain on collector surfaces after bakeout (**Figure 11**). The residual number of the individual compounds was determined to be about 2.40×10^{-15} mol (2.4 fmol), whereas more volatile unmodeled compounds, including the breakdown products expected of amino acids, were expected to reduce to equivalent or lower levels. The compound having the highest heat of adsorption of the set, *n*-pentacosane, left the highest amount residue (~12%; **Supplementary Material**), which biased the average. In any case, it is expected that the amount of remaining contamination will be highly dependent upon the starting amount of material.

The initial conditions for the model assumed a worst-case, unrealistic scenario: a uniform monolayer of semi-to non-volatile molecules per simulation, which is orders of magnitude denser than expected for precision cleaned surfaces. However, the modeling revealed two significant findings: 1) bakeout resulted in a full order of magnitude

decrease on average for the wide range of molecules having different heats of adsorption, and 2) most of the molecules were entirely gone from the collector surface after bakeout with exception to *n*-pentacosane that biases the average with 12% remaining.

In contrast to the CTSP model, the traditional physics model having lower fidelity adsorption-desorption physics indicated a remarkable one part per trillion of the contaminants remained. Both models assumed the same initial conditions. Starting from effectively a monolayer height of molecules covering the collector at launch, the final remaining surface mass is approximately 2×10^{-13} g, a reduction by 10^{12} after 60 min of bakeout. These results demonstrate the standard physics model's divergence from reality when molecular coverage approaches monolayers or less (**Supplementary Material**).

Probability of Ice Particles Transporting Contaminants to the Instrument Inlet

Ice-Driven Molecular Transport

Assuming a 2-m^2 collector surface area, and approximately 100% collection efficiency, and an initial monolayer of *n*-pentacosane as a representative molecular contaminant on the collector surface, the total number of moles collected would be 6.35×10^{-13} mol. The monolayer coverage was 1.37×10^{-10} mol/cm^2. Given the calculated distorted particle impact ratio at shatter (**Supplementary Material**), the total impacted area for 50 µL of ice was 4.64×10^{-3} cm^2 (2.32×10^{-7} of the total area of the collector). For the same reasons mentioned earlier (*Model of the In-Cruise Collector Bakeout Activity*), this scenario is informative but unrealistic.

Following a 300°C-bakeout of the collector that started with a monolayer (*Decontamination Efficacy of an In-Cruise Collector Bakeout*), CTSP model results indicated 2.40×10^{-15} mol of individual contaminant compounds remaining on the collection, given the above impact area, 5.57×10^{-22} mol of contaminant molecules may transfer to the collector. If less ice sample impacts the collector, the molecular contaminant transport to the instrument inlet will be proportionally less.

Ice-Driven Dust and Microbial Particle Transport

Initial conditions of level 100 cleanliness for the collector surfaces corresponds to a surface area coverage of 2.19 parts per million (fractionally 2.19×10^{-6} of the surface). Assuming the full diameter of the particle as the impact cross-section, the total impacted area for 50 µL of ice particles will be 46.7 cm^2, and the fraction of the collector impacted by ice particles is 2.33×10^{-3}. Thus, the probability of dust particle contamination transported to the detector by an ice particle is 5.1x10-9. Depending on dust particles composition, dust particles entering the instrument inlet may or may not impact science hardware and measurements.

For particulates that are microbial in nature (cells, spores, cell parts) initial conditions were set at a nominal viable bioburden level of 300 colony-forming units per m^2. Further, it was assumed that this bioburden level was 1% of the total
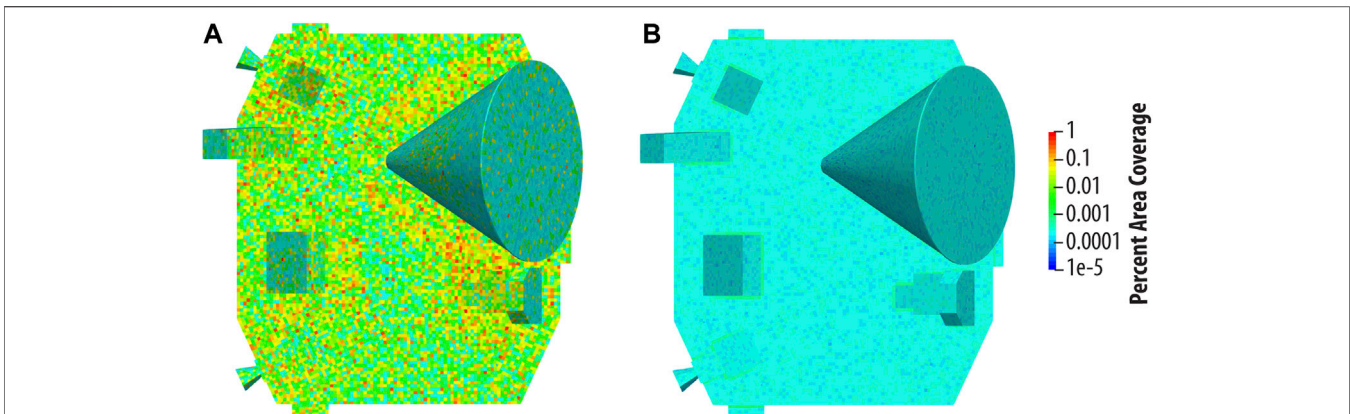
FIGURE 10 | Comparison of the particle distributions on the spacecraft after ascent, without a barrier **(A)** and with the barrier **(B)**. In both cases, the PAC numbers at time zero were set to 2×10^{-4} PAC. In the no-barrier case **(A)**, the fairing cleanliness was set to the nominal cleanliness level specified for a fairing. In the barrier case **(B)**, the barrier cleanliness was specified at the same level as the spacecraft surface. During launch, particles are released from the hardware due to the vibration and acceleration. These then are redistributed following the physical forces acting on each particle following the changing conditions of acceleration and venting on launch. In the no barrier case, the spacecraft becomes more contaminated with particles from the fairing, which will include a viable microbes attached from non-bioburden reduced fairing. In the barrier case, particles are lost from the spacecraft due to the launch loads, and any particles landing on the spacecraft are limited to those from the bioburden reduced barrier interior. As a result, the contamination level of the spacecraft will decrease in the case of the barrier.
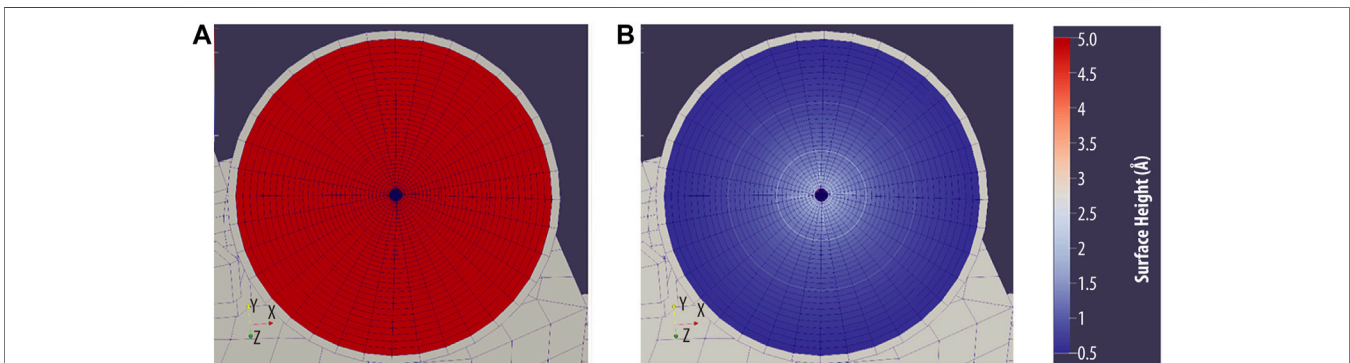
FIGURE 11 | Views into the collector cone showing the higher fidelity molecular model results of the in-cruise collector bakeout after a simulated in flight bake out. A monolayer of molecules (5 Å) present at 0 min **(A)** was reduced to an average of 12.9% of the original loading after 60 min of heating **(B)** at high temperature. The level of reduction is dependent upon the composition and loading of the molecular contamination on the collector. The fixed test case molecular contamination composition was four common molecular contaminants in equal volumetric proportion. The rest of the spacecraft is not included in this molecular transport model run as there was no detectable contribution from the other surfaces in full spacecraft modeling. The color scale is linear between 0.5 and 5 Å. The lower fidelity constant heat of vaporization calculations for the same bake out result in a less physical near complete loss of the molecular contamination.

burden of viable and non-viable microbes and their parts. The calculated probability of a microbe or its parts on the collector surface being transported to the instrument inlet was 4.39×10^{-10}, which is exceptionally low and will have no impact on the science measurements. Further, this calculation does not take into account possible degradation and loss of microbial particles during the collector bakeout, which has the potential to improve the probability and making even less likely that terrestrial microbial particulates will be dislodged and transported to the instrument inlet during plume sampling.

DISCUSSION

This study demonstrated the practicality of a fully encapsulating spacecraft-level barrier for extreme contamination control and the necessary application of contamination transport modeling for particles and molecules using high-fidelity physics for meeting contamination requirements traceable to mission science.

The collector-cover labyrinth seal effectively mitigates all particle intrusion into the cone even without a purge gas. The purge gas having part-per-trillion purity with respect to non-volatile residues and target compounds is obtainable using point-

of-use filtration and will preserve the cleanliness of the collector until the purge is exhausted in the vacuum of space. The purged barrier will significantly limit the partial pressure of molecular contaminants in the large barrier volume to which the labyrinth seal is exposed. Continuous purge of the barrier will serve to dilute any evolved contaminants being released from spacecraft surfaces inside the barrier. The barrier pressure relief vent will minimize the probability of infiltration of contamination into the barrier during launch assent. As a result, the efficacy of the collector's labyrinth seal situated inside the in the purged barrier will be higher than in the absence of the barrier.

The barrier effectively acts to provide a significant degree of isolation for most of the spacecraft from the fairing and the launch pad environments. Particulate material from outside of the barrier will be effectively excluded from the inner barrier volume.

The bakeout allows meeting the DRM molecular contamination requirements despite the unrealistically conservative contamination component distribution in the simulated system. After bakeout, the total surface contamination mass left on the largest portion of the collector is 1.4×10^{-5} g distributed over a surface area of 2 m^2, giving an average surface density of 7×10^{-10} g/cm^2. As this residue is primarily nC25, the residual molar surface density was 2.0×10^{-12} mol/cm^2. The higher fidelity of the material-material interactions significantly reduced the over-estimation of the efficacy of the cruise bake out bringing it more in line with actual physical bake out behavior.

The chosen model assumed that 25% of the surface contamination was the nC25, which is an unrealistically high fraction for any individual compound in a contamination sample. Most residual contamination samples show a significantly broader distribution of molecules resulting in a larger number of smaller individual species concentrations. Assuming a large sample collection of 50 μL, a worst-case scenario for contamination transport, plume ice impact area on the collector would be 2.3×10^{-3} cm^2 and the amount of nC25 contamination would be 5.57×10^{-22} mol. Scaled to the 2 μL minimum expected sample volume, this worst-case model meets the contamination requirement (CNTM-2) of less than 20 fmol for individual lipid-hydrocarbon compounds. Accordingly, it is expected that amino acid contamination will be at the same level or less meeting contamination requirement CNMT-1.

Contamination requirements should be traceable to L1 science requirements and mission implementation. The mission design and implementation must also include verification and validation of contamination control measures taken during build, integration, launch processing, launch, and cruise. This will increase the likelihood of successfully meeting the requirements for science operations.

The behavior of molecules on surfaces are different from molecules in bulk. Improved analysis techniques can overcome the limitations of current methods for evaluating contamination transfer from surfaces having a monolayer or less contaminants. This approach enables adaptation of a set of mitigation strategies in mission design, which include and expand upon traditional bulk transfer approaches, to ensure that the cleanliness requirements post launch are both feasible and achievable. When applied to launch and cruise operations of the reference mission, the model revealed that cleaning of spacecraft, ultra-cleaning of critical surfaces in the sample path, covering on the

sample collector, and purging the collector with ultra-high purity N$_2$ gas, were still not sufficient to meet the contamination requirements necessary for expected instrument performances at Enceladus. The model demonstrated that both a full spacecraft barrier that protects the cleaned spacecraft during launch operations and a high temperature bakeout of the collector with cover open during cruise are necessary to ensure the extremely low levels of contamination required by life-detection science measurements.

CONCLUSION

The use of a bio-molecular barrier protects the spacecraft from known external contamination sources and mitigates any unknown sources, significantly reducing contamination risk and its potential impact on mission science. Additionally, high temperature bakeouts during mission cruise have been shown to reduce contamination to nearly undetectable levels. Computational fluid dynamics in contamination transport modeling under continuum flow conditions can significantly advance the fidelity of contamination transport. The computational model developed in this study provides accurate prediction of transport for very low contamination at the monolayer and sub-monolayer levels of surface contamination. The models account for aerodynamic, electrostatic, and gravitational forces that vary spatially and temporally with complex spacecraft geometries. They apply detailed surface chemistry and physics (i.e., sorption behavior) to provide accurate contamination predictions for transport, adsorption, and desorption of very low levels of surface contaminants. The modeling innovations of this study provide the key qualitative and quantitative insight needed to determine how effective contamination mitigation approaches are for future mission designs.

In life-detection missions, exceedingly small amounts of target compounds can make or break a mission. It is critical that normally ignored minor contaminant contributions be evaluated with higher fidelity as part of the mission design process. Based on contamination transport modeling conducted in this study and application of bio-molecular barriers and in-flight bakeouts, reaching the cleanliness levels required to meet the science requirements is practical and reasonably cost effective.

DATA AVAILABILITY STATEMENT

The original contributions presented in the study are included in the article/**Supplementary Material**, further inquiries can be directed to the corresponding author.

AUTHOR CONTRIBUTIONS

JE and RG led the study design. JE and AS managed the project. JE prepared the manuscript for publication. RG oversaw the barrier technology development. JC provided critical data input to the CTSP modeling, performed data analyses, and provided input to manuscript for the modeling aspects of the study. ES led the barrier design, performed data analyses, and provided inputs to

manuscript for the barrier aspects of the study. AS oversaw the compilation of results. CL oversaw the modeling technology development. CL and TE provided contamination engineering inputs to all aspects of the study and related inputs for the manuscript. FK and DK compiled the requirements definitions, ensured requirements were met by study products, and oversaw the system engineering aspects of the barrier and model application. JE, RG, AD and CM provided science, design reference mission, and other life-detection mission concept considerations throughout the technology developments. All authors contributed to the article and approved the submitted version.

SUPPLEMENTARY MATERIAL

The Supplementary Material for this article can be found online at: https://www.frontiersin.org/articles/10.3389/frspt.2021.734423/full#supplementary-material

Table S1 | Study objectives.

Table S2 | Study ground rules.

Table S3 | Level-1 LVE definitions (requirements) traceable to GR-2, GR-3, and GR-15.

Table S4 | Level-2 contamination requirements (CNTM) traceable to SCI-1 and SCI-2 from the DRM (Table 1).

Table S5 | Level-2 barrier design (BD) requirements and goals.

Table S6 | Launch ascent venting environment pressure and vent rate.

Table S7 | Level-3 Derived Requirements.

video S1 | Barrier demonstration RTG View.

Video S2 | Barrier demonstration Antenna View.

Data Sheet 1 | Supplemental on Bio-Molecular Barrier.

Data Sheet 2 | Supplemental on Model.

REFERENCES

Adams, E., McKay, C., Ricco, A., Gold, R. E., Bonaccorsi, R., et al. (2018). "EFun: the Plume Sampling System for Enceladus," in 42nd COSPAR Scientific Assembly, Pasadena, California, USA, 14-22 July 2018. Available at: https://ui.adsabs.harvard.edu/abs/2018cosp...42E..22A/abstract#:~:text=EFun%20is%20the%20enabling%20technology,plume%20and%20determine%20Enceladus'%20habitability.

Brieda, L. (2019). Numerical Model for Molecular and Particulate Contamination Transport. *J. Spacecraft Rockets* 56, 485–497. doi:10.2514/1.a34158

Brunauer, S., Emmett, P. H., and Teller, E. (1938). Adsorption of Gases in Multimolecular Layers. *J. Am. Chem. Soc.* 60, 309–319. doi:10.1021/ja01269a023

COSPAR Policy on Planetary Protection (2020). COSPAR Policy on Planetary Protection. *Space Res. Today* 208, 10–22. Available at: https://cosparhq.cnes.fr/assets/uploads/2020/07/PPPolicyJune-2020_Final_Web.pdf.

Dworkin, J. P., Adelman, L. A., Ajluni, T., Andronikov, A. V., Aponte, J. C., Bartels, A. E., et al. (2018). OSIRIS-REx Contamination Control Strategy and Implementation. *Space Sci. Rev.* 214, 19. doi:10.1007/s11214-017-0439-4

Eigenbrode, J. L., Gold, R. E., McKay, C. P., Hurford, T., and Davila, A. (2018). "Searching for Life in an Ocean World: The Enceladus Life Signatures and Habitability (ELSAH) mission Concept," in 42nd COSPAR Scientific Assembly. Held, Pasadena, California, USA, 14-22 July 2018. Available at: https://ui.adsabs.harvard.edu/abs/2018cosp...42E.969E/abstract.

Hand, K. P., Murray, A. E., Darvin, J. B., Brinckerhoff, W. B., Christner, B. C., Edgett, K. S., et al. (2017). *Report of the Europa Lander Science Definition Team*. NASA. Available at: https://europa.nasa.gov/system/downloadable_items/50_Europa_Lander_SDT_Report_2016.pdf.

MacKenzie, S. M., Neveu, M., Davila, A. F., Lunine, J. I., Craft, K. L., Cable, M. L., et al. (2021). The Enceladus Orbilander Mission Concept: Balancing Return and Resources in the Search for Life. *Planet. Sci. J.* 2, 77. doi:10.3847/psj/abe4da

McKay, C. P., Stoker, C. R., Glass, B. J., Davé, A. I., Davila, A. F., Heldmann, J. L., et al. (2013). The Icebreaker Life Mission to Mars: A Search for Biomolecular Evidence for Life. *Astrobiology* 13, 334–353. doi:10.1089/ast.2012.0878

National Academies of Sciences, Engineering, and Medicine (2018). *Review and Assessment of Planetary Protection Policy Development Processes*. Washington, DC: The National Academies Press. doi:10.17226/25172

National Academies of Sciences, Engineering, and Medicine (2020). *Assessment of the Report of NASA's Planetary Protection Independent Review Board*. Washington, DC: The National Academies Press. doi:10.17226/25773

Porco, C. C., Dones, L., and Mitchell, C. (2017). Could it Be Snowing Microbes on Enceladus? Assessing Conditions in its Plume and Implications for Future Missions. *Astrobiology* 17, 876–901. doi:10.1089/ast.2017.1665

Regberg, A. B., Castro, C. L., Connolly, H. C., Davis, R. E., Dworkin, J. P., Lauretta, D. S., et al. (2020). Prokaryotic and Fungal Characterization of the Facilities Used to Assemble, Test, and Launch the OSIRIS-REx Spacecraft. *Front. Microbiol.* 11, 530661. doi:10.3389/fmicb.2020.530661

Reh, K., Spilker, L., Lunine, J. I., Waite, J. H., Cable, M. L., Postberg, F., and Clark, K. (2016). Enceladus Life Finder: The Search for Life in a Habitable Moon. IEEE Aerospace Conference Proceedings. Big Sky, MT, USA. 5-12 March 2016. doi:10.1109/AERO.2016.7500813

Steddum, R. E. (1971). *Characteristics of Water Sprays under Vacuum Conditions*. LSU Historical Dissertations and Theses, 116. Available at: https://digitalcommons.lsu.edu/gradschool_disstheses/2013/.

Turtle, E. P., Barnes, J. W., Trainer, M. G., and Lorenz, R. D. (2018). "'Dragonfly: *In Situ* Exploration of Titan's Organic Chemistry and Habitability'," in 49th Lunar and Planetary Science Conference, Teh Woodlands, TX, 1641. Available at: https://www.hou.usra.edu/meetings/lpsc2018/pdf/1641.pdf.

Williford, K., Farley, K., Stack, K., Allwood, A., Beaty, A., Beegle, L., et al. (2018). "The NASA Mars 2020 Rover Mission and the Search for Extraterrestrial Life," in *In from Habitability to Life on Mars* (Elsevier), 275–308. Available at: https://doi.org/10.1016/B978-0-12-809935-3.00010-4. doi:10.1016/B978-0-12-809935-3.00010-4

Willson, D., Gold, R., Slone, D., Bonaccorsi, R., Mathias, D., and McKay, A. C. P. (2017). "Catching Life in the Icy Plumes of Europa and Enceladus," in Astrobiology Science Conference 2017, Mesa, AZ, 3663. Available at: https://www.hou.usra.edu/meetings/abscicon2017/pdf/3663.pdf.

Conflict of Interest: JC was employed by Peraton, Inc.

The remaining authors declare that the research was conducted in the absence of any commercial or financial relationships that could be construed as a potential conflict of interest.